

JCTC

Journal of Chemical Theory and Computation

Using Electronic Energy Derivative Information in Automated Potential Energy Surface Construction for Vibrational Calculations

Manuel Sparta,^{*,†} Mikkel B. Hansen,[†] Eduard Matito,^{†,‡} Daniele Toffoli,^{†,§} and Ove Christiansen[†]

The Lundbeck Foundation Center for Theoretical Chemistry, Center for Oxygen Microscopy and Imaging, Department of Chemistry, University of Aarhus, Langelandsgade 140, DK-8000 Aarhus C, Denmark, Institute of Physics, University of Szczecin, Wielkopolska 15, 70-451 Szczecin, Poland, and Department of Chemistry, Middle East Technical University, 06531 Ankara, Turkey

Received May 4, 2010

Abstract: The availability of an accurate representation of the potential energy surface (PES) is an essential prerequisite in an anharmonic vibrational calculation. At the same time, the high dimensionality of the fully coupled PES and the adverse scaling properties with respect to the molecular size make the construction of an accurate PES a computationally demanding task. In the past few years, our group tested and developed a series of tools and techniques aimed at defining computationally efficient, black-box protocols for the construction of PESs for use in vibrational calculations. This includes the definition of an adaptive density-guided approach (ADGA) for the construction of PESs from an automatically generated set of evaluation points. Another separate aspect has been the exploration of the use of derivative information through modified Shepard (MS) interpolation/extrapolation procedures. With this article, we present an assembled machinery where these methods are embedded in an efficient way to provide both a general machinery as well as concrete computational protocols. In this framework we introduce and discuss the accuracy and computational efficiency of two methods, called ADGA[2gx3M] and ADGA[2hx3M], where the ADGA recipe is used (with MS interpolation) to automatically define modest sized grids for up to two-mode couplings, while MS extrapolation based on, respectively, gradients only and gradients and Hessians from the ADGA determined points provides access to sufficiently accurate three-mode couplings. The performance of the resulting potentials is investigated in vibrational coupled cluster (VCC) calculations. Three molecular systems serve as benchmarks: a trisubstituted methane (CHFCIBr), methanimine (CH₂NH), and oxazole (C₃H₃NO). Furthermore, methanimine and oxazole are addressed in accurate calculations aiming to reproduce experimental results.

1. Introduction

During the past few years, accurate calculation of vibrational spectra and vibrational corrections to molecular properties have become increasingly feasible due to the development of ad hoc efficient computational methods. Restricting

attention to time-independent explicit wave function methods, the vibrational self-consistent field (VSCF)^{1–4} method is the first to be mentioned. In a VSCF calculation a mean-field description of the multimode dynamics is achieved. In analogy with the Hartree–Fock method of electronic structure theory, a VSCF calculation may serve as the starting point for more elaborate correlated calculations. For instance, explicit mode–mode correlation may be accounted for with vibrational Møller–Plesset perturbation theory (VMP, by some denoted correlation-corrected VSCF, cc-VSCF),^{5–10}

* To whom correspondence should be addressed. E-mail: msparta@chem.au.dk.

[†] University of Aarhus.

[‡] University of Szczecin.

[§] Middle East Technical University.

vibrational configuration interaction (VCI),^{2,3,11–16} and vibrational coupled-cluster (VCC),¹⁴ and for the latter two vibrational response theory can be applied to calculate excitation energies and properties.^{17,18}

A fundamental prerequisite for the accuracy of any vibrational calculation is the availability of a precise representation of the anharmonic part of the PES. This means that a sufficiently large portion of the Born–Oppenheimer (BO) hypersurface has to be sampled with electronic structure methods, which represents one of the bottlenecks in molecular vibrational dynamics. In fact, one should notice that the dimensionality of the hypersurface grows linearly with the number of atoms in the molecule, and hence, the calculation of a fully coupled PES is prohibitive except for the smallest molecules.

To overcome this problem, the full-dimensional PES can be approximated as a sum of potential energy functions (PEFs) of lower dimensionality and high-order mode couplings are included in a hierarchical way. In the vibrational context, this approximation goes under the name of *n*-mode representation of the potential. It was originally suggested and implemented by Carter et al. up to four-mode couplings,¹⁹ while around the same time, a similar approach restricted to two-mode couplings was suggested and since used extensively by Gerber and co-workers.^{6,20} The restricted mode-coupling approach is becoming a standard way for constructing accurate approximate PESs and has been generalized and extended in various ways and combined with various techniques for obtaining efficiency in the calculations.^{6,15,21–27} At least for fairly rigid molecules the restricted mode-coupling expansion of the potential converges fast with the mode-coupling level and inclusion of up to the three-mode-coupling terms provides sufficiently accurate fundamental vibrations. However, inclusion of three-mode couplings soon becomes computationally costly as the size of the molecular system is increased.

Recently, we implemented an adaptive density-guided approach (ADGA) for accurate and flexible representation of the potential energy functions, (PEFs) relevant to quantum dynamics calculations.²⁸ The method allows for a dynamical and automatic generation of the grid of evaluation points for each PEF included in the approximate representation of the fully coupled PES. The term “dynamical” relates to the adaptive strategy for determining the grid boundaries. This is opposed to a “static” determination of the grid of points, where the grid boundaries are specified by the user on input, see, e.g., ref 25. In the ADGA, the densities of the vibrational wave functions are used to guide the dynamic generation of the grids of evaluation points with respect to both the size of the grid and the mesh of evaluation points. Subsequently, the procedure was improved by adding multilevel or multitiresolution capabilities, i.e., information from single-point calculations executed with different electronic structure methods are combined to increase the accuracy and/or reduce computational cost.²⁹ The attractiveness of adaptive procedures has also been emphasized in a quite different context by Iyengar and co-workers.^{30,31} In ref 31 it is shown how the use of a partial nondirect product grid in an adaptive scheme to construct PESs has a significant effect on the

computational accuracy and efficiency. As the appropriate definition of nondirect grids is not clear in this context, we use direct product grids for our PEFs. We also point out that Rauhut¹⁵ discussed iterative approaches as means of error control and, in conjunction with other clever tricks, reported huge computational savings. Finally, a completely different approach toward building up the PES is the use of neural networks as pursued by Manzhos and Carrington.^{32,33}

In a concurrent project, our lab has developed a procedure for the generation of molecular PESs which integrates the aforementioned restricted mode-coupling representation of the PES with efficient use of derivative information by means of a modified Shepard (MS) interpolation/extrapolation. In particular, the method aims at calculating higher mode couplings by extrapolation of lower mode couplings in a grid-based approach. The method does not require any a priori knowledge of the potential and has, using second-order derivatives, been shown to give an accuracy competitive with that of the explicitly calculated higher order mode-coupling PES. Using only gradients already leads to significant improvements. For a detailed explanation and an overview on the use of derivatives information in the PES construction we refer to ref 36 and references therein as well as Dawes et al.^{34,35} for interesting alternative approaches and further references.

In this article we integrate the use of the MS interpolation/extrapolation with the multilevel implementation of the ADGA. This carries both theoretical and technical challenges. First, the procedures for interpolation and extrapolation were found solid and useful when based on rather dense and homogeneous grids constructed with a “static” approach; within the ADGA framework, the iterative procedure provides relatively coarse and dishomogeneous grids; hence, both accuracy and efficiency must be thoroughly investigated. From the implementational point of view, it is not unique how to define and use the interpolating functions during the iterative procedure nor is the resulting effect on the convergence rate clear. Once these issues are investigated and addressed, the goal is (i) to achieve a faster convergence of the iterative approach and (ii) establishing higher order extrapolated PEFs from parental lower order mode couplings converged with the ADGA as accurate but low-cost approximations to explicitly calculated higher order terms.

From these general aspects we can define concrete PES construction protocols, for instance, ADGA[2gx3M] where the ADGA recipe is used (with MS interpolation) to automatically define accurate representation for up to two-mode couplings, while the MS extrapolation trick based on gradients is used to construct the three-mode couplings. Alternatively, if both gradient and Hessian are used we will refer to the PES with the code ADGA[2hx3M]. As a further example, a 2M potential where the one mode part is explicitly constructed and the two-mode couplings are extrapolated using both gradients and Hessians will be referred by ADGA[1hx2M]. Certainly, the possibility to obtain three-mode couplings with only two-mode grids is a unique opportunity. In passing we note a very interesting procedure recently developed by Rauhut:³⁷ A semiempirical method is adjusted for the particular molecule and the particular set

of one- and two-mode calculation points. Using this adjusted and fast semiempirical method provides another way of constructing three-mode couplings without the explicit ab initio electronic structure calculations of the potentially large number of three-mode grids.

While calculation of the PES is a costly procedure, calculation of the anharmonic wave function for a given potential can also be extremely costly as the size of the molecule increases. Recently, some of us derived concrete optimal formal scalings and accompanying implementations for vibrational wave function methods such as VCC and VCI.^{4,38} In this study our main vibrational wave function method is the recently developed VCC[2pt3] approach,³⁹ which in the framework of VCC response theory gives a full description of two-mode couplings and a perturbational motivated approximate inclusion of three-mode excitations. For each state calculated, VCC[2pt3] comes with a modest cubic scaling with respect to the number of degrees of freedom.³⁹ Clearly, the combined use of, e.g., ADGA[2gx3M] and VCC[2pt3] is natural as these methodologies are unique in providing a computationally realistic inclusion of three-mode couplings in the PES and wave function parts, respectively. Thus, their combined use allows for accurate calculations on larger molecules where calculations otherwise would have to be limited to approaches including only up to two-mode couplings. As a further point, ADGA has been shown to lead to reduced scaling also in the wave function part due to its ability to provide compact representation of the PES.⁴

The paper is organized as follows. In section 2 we describe the ADGA algorithm used for generation of the grids of evaluation points relating it to previous works as well as the features and implementation of the MS procedures. Furthermore, the way the two concepts are integrated is fully accounted for. A brief summary of the computational details follows in section 3. The results of the benchmark calculations are given in section 4 and organized as follows: first, we present the convergence properties of the algorithm described by means of a systematic survey on 3 smaller molecules (trisubstituted methane, methanimine, and oxazole). Second, we apply the knowledge gained to attempt an accurate calculation of the vibrational spectra of methanimine and oxazole with high-level electronic structure methods. Finally, conclusions and perspectives are given in section 5.

2. Description of the Method

2.1. Vibrational Hamiltonian and Potential Energy Operator. Vibrational energies and vibrational contributions to molecular properties are obtained from solution of the Born–Oppenheimer vibrational Schrödinger equation. The Hamiltonian in mass-weighted rectilinear normal coordinates ($q_m \in \mathbf{Q}$) can be written as

$$H = T(\mathbf{Q}) + V(\mathbf{Q}) \quad (1)$$

where $T(\mathbf{Q})$ is the kinetic energy operator (either in the Watson form⁴⁰ or simply as a sum of $-(1/2)(d^2/dq_m^2)$ terms; for details and further references we refer to our previous ref 25). $V(\mathbf{Q})$ is the BO potential energy term.

In order to reduce the large dimensionality of the problem associated with computation of the potential energy surface the restricted mode-coupling representation of the fully coupled potential is adopted.^{6,15,19,21,23} One starts by defining a set of potential energy functions (PEFs) which include the coupling among a subset n of the M vibrational degrees of freedom

$$\begin{aligned} V^{m_i} &= V(0, \dots, 0, q_{m_i}, 0, \dots, 0) \\ V^{m_i, m_j} &= V(0, \dots, 0, q_{m_i}, 0, \dots, 0, q_{m_j}, 0, \dots, 0) \end{aligned} \quad (2)$$

and so forth up to V^{m_1, m_2, \dots, m_M} , the fully coupled potential, $V(\mathbf{Q})$. In eq 2 $m_i \neq m_j$. For the sake of simplicity the set of modes (referred to as a mode combination, MC, hereafter) defining the particular PEF are collected in an n -dimensional vector \mathbf{m}_n . In this way, an n -dimensional PEF is denoted as $V^{\mathbf{m}_n}$. Furthermore, one notes that by summing over all MCs, overcounting is introduced since each n -dimensional PEF includes all the lower dimensional PEFs corresponding to the set of $\mathbf{m}_n' \subset \mathbf{m}_n$. In order to avoid overcounting, potentials $\bar{V}^{\mathbf{m}_n}$ are conveniently introduced (see, e.g., ref 23 for details) such that

$$V = \sum_{\mathbf{m}_n \in \text{MCR}\{V\}} \bar{V}^{\mathbf{m}_n} \quad (3)$$

where MCR is a mode-combination range, the set of MCs we want to include in the potential.

Within this framework we developed some efficient computational protocols. The overall setup is rather general. For a given mode-combination level n , all the n -dimensional PEFs, $V^{\mathbf{m}_n}$, are sampled in a set of grid points by means of ab initio electronic structure calculations. An analytic representation is then obtained by fitting each of the PEFs to a multivariate polynomial in frequency-scaled mass-weighted normal coordinates (for more details we refer to ref 25). To appreciate the overall setup in this paper we shall now briefly describe the adaptive density-guided approach for construction of the PES.

2.2. Adaptive Density-Guided Approach for Construction of the PES. The basic ideas of ADGA²⁸ are (i) the boundaries of the sampling grids are determined by the spatial extension of the vibrational wave functions studied and therefore depend naturally on the specific chemical problem under investigation, (ii) each of the PEFs is initially explored with a “minimal” sampling grid, the mesh of the grid is iteratively refined until the reference vibrational wave function calculation is stable toward further extension within a threshold, and (iii) vibrational wave functions are used to construct vibrational densities (ρ) which are used as key quantities in the construction of $\rho \times V$ “energy-like” contributions. These contributions help to identify the importance of each mode coupling as well as the optimized grid mesh for its description.

The PES construction and wave function density calculation now become interdependent of each other. In this context, our recently proposed fast VSCF algorithm is useful due to the (possibly) large number of VSCF optimizations required.⁴ The original papers detail the used densities, and

we note only that the user in input specifies the vibrational levels taken into account in the density calculation and that the VSCF one-mode densities integrate to one over the full one-mode configuration space. This feature is used to ensure that the grid boundaries for construction of the PES covers the space explored by the wave function.

In the ADGA for PES construction grid points are systematically added until convergence: The n th iteration starts with evaluation of the PEFs in correspondence to the list of points generated in the $(n - 1)$ th iteration. An analytical representation of the $V^{\mathbf{m}, n\text{th}}$ terms is provided via a polynomial fitting (superscript n th refers to the n th iteration). The potential is then used in a VSCF calculation for the ground vibrational state, and the VSCF models are then used to construct the vibrational density $\rho_{av}^{n\text{th}}$ for mode q_m . The grid is then considered as composed of subsectors (wherein 1D a subsector is defined as the interval between two adjacent sampling points). For each subsector we can define an “energy-like” contribution, $(\rho V)_i^{n\text{th}} = \int_{\Omega_i} \rho_{av}^{n\text{th}}(q_m) V^{\mathbf{m}, n\text{th}}(q_m) dq_m$, where Ω_i denotes the i th interval. A further testing point is requested at the middle point of the subsectors for which the condition

$$\frac{(\rho V)_i^{n\text{th}} - (\rho V)_i^{(n-1)\text{th}}}{(\rho V)_i^{n\text{th}}} < \varepsilon_{\text{rel}} \quad (4)$$

is not fulfilled. Here, $(\rho V)_i^{(n-1)\text{th}}$ is taken equal to zero at the first iteration. An interval where the relative variation of the integral value $(\rho V)_i$ between two iterations is found to be larger than a specified threshold (usually of the order of 1%) is further subdivided with addition of a new testing point. Furthermore, intervals with a small contribution to the energy are not further subdivided, regardless of the relative error computed by means of eq 4. In particular, a subsector is not further divided if the conditions

$$(\rho V)_i^{n\text{th}} - (\rho V)_i^{(n-1)\text{th}} < \varepsilon_{\text{abs}} \wedge (\rho V)_i^{n\text{th}} < \varepsilon_{\text{abs}} \quad (5)$$

are fulfilled, with ε_{abs} being usually on the order of 10^{-6} au. The n th iteration ends with the definition of the new subsectors, calculation and storage of the integrals to be used in the subsequent iteration, and a list of new sampling points is compiled.

The ADGA converges hierarchically up to a user-specified maximum mode-combination level, i.e., monodimensional PEFs are converged before the bidimensional ones and so forth. The adaptive construction of the n -dimensional grids is a straightforward generalization of the procedure outlined above:⁴¹ the multidimensional grid domains are partitioned in subsectors defined by 2^n adjacent points (see ref 28), the convergence criteria are n -dimensional generalization of the criteria outlined above, and the n -mode densities for construction of the $(\rho V)_i$ quantities are taken to be a direct product of the converged one-mode densities $(\rho(q_m))$.

In a multilevel or multiresolution procedure for PES construction, PEFs computed with different methods and/or approximations (electronic structure methods, basis sets, analytic representations, and electronic structure programs) are combined to obtain a hybrid PES.^{15,24,42–44} We refer to

ref 24 for an exhaustive discussion of this formalism adapted to the intrinsic mode-coupling framework. In the multiresolution implementation, the ADGA is used for construction of the various PEFs entering in the final PES allowing for the following two options: (i) the PEFs for a given mode coupling term can be combined to include extrapolation procedures and/or linear corrections and (ii) a PES with a lower maximum mode-combination level can be corrected adding higher mode-combination terms from PEFs constructed with computationally less expensive electronic structure methods. In passing, we note that the use of a multiresolution procedure is well suited for a preoptimization of the grid boundaries. A detailed description of the implementation and integration with the ADGA can be found in ref 29.

2.3. Use of Derivative Information. The quartic force field representation of the PES is an obvious example of the use of derivatives in PES constructions. However, such a representation relies on a local Taylor series expansion, and thus, the description of the potential may not be accurate in regions far from the ground state equilibrium geometry. To overcome this problem, the modified Shepard interpolation has been adopted by several authors. Yagi et al.^{45–47} showed that with some knowledge of the vibrational structure of the molecule, one might obtain a very accurate PES by using a few Taylor expansions centered in the vicinity of higher mode-coupling regions. This method proved very effective even for PESs with moderately strong mode couplings. Other studies have also emphasized that derivative information can be very useful if one has an effective method to generate the candidate points.^{48,49}

Recently, our group developed a similar procedure for generation of the PES following a different spirit: rather than aiming at a PES described by a few high-order Taylor expansions suitably located, the focus was on a dense grid using in this way many low-order Taylor expansions. The approach does not require prior knowledge about the PES and simplifies input preparation. Such an approach was integrated with the restricted mode-coupling representation, thus producing a natural extrapolation scheme for higher mode couplings based solely on calculations on grids for lower mode couplings. By merging both techniques one introduces additional steps in the hierarchical construction of the PES, e.g., three-mode-coupling potentials extrapolated from two-mode-coupling ones using gradients only, here denoted 2gx3, or both gradients and Hessians, here denoted 2hx3, to provide accuracies between the 2M and 3M potentials.³⁶ In addition, yet within the restricted mode-coupling representation, derivative information can be used to interpolate within the same mode-coupling level to provide additional points before a polynomial fitting.³⁶ We shall now describe the interpolation step, how it can be integrated with ADGA, and how a practical extrapolation step can be defined.

2.3.1. Interpolation. In a standard MS interpolation, the interpolated energy value for the point \vec{q} , is obtained as a weighted sum of local Taylor series (one for each expansion point)

$$\tilde{f}(\vec{q}) = \sum_i w_i(\vec{q}) f_i(\vec{q}) \quad (6)$$

$$f_i(\vec{q}) = \sum_{j=0}^{j=m} \left[\frac{1}{j!} ((\vec{q} - \vec{q}_i) \cdot \vec{\nabla}_{\vec{x}})^j f(\vec{x}) \right]_{\vec{x}=\vec{q}_i} \quad (7)$$

where m is the order of the Taylor series and \vec{q}_i are the expansion points. Having usually available only low derivative expansions ($m = 1$ or 2), we investigate in this work whether, in the case of reducing the density of grid, such low-order Taylor series still produce sensible interpolated values. Another important factor for the accuracy of the MS interpolation approach is the weight factors chosen. It is customary to take a function of the inverse of distance as a weight factor. In particular, high powers of the inverse of the distance have been shown to be highly effective in the construction of interpolated values (for the notation used here see ref 36)

$$w_i(\vec{q}) = \frac{\|\vec{q}_i\|^{-2p}}{\sum_j \|\vec{q}_j\|^{-2p}} \quad (8)$$

Here $p = 1, 2, \dots, p = 3N - 6$ has been recommended in MSI interpolations⁴⁶ but should of course be modified according to the dimensionality of the particular mode coupling.

2.3.2. Interpolation Combined with ADGA. During a standard ADGA iteration, the energy information collected from the set of single-point calculations undergoes a polynomial fitting. Especially in the early iterative cycles, the number of single-point calculations, and hence property values, is low and property derivatives are useful for defining a finer grid of points, which combines both calculated and interpolated points to be fitted.

In Figure 1, the strategy for the positioning of the fine grid of points to be interpolated is depicted in the case of a monodimensional surface. For each sector (the interval between two adjacent sampling points x_i and x_{i+1} , blue diamonds) two points to be interpolated are defined at $x_i + a(x_{i+1} - x_i)$ and $x_i + (1.0 - a)(x_{i+1} - x_i)$, where a is a user-defined parameter. For the monodimensional surfaces, two additional interpolation points are added outside the grid boundaries at $x_{\text{first}} - a(x_{\text{second}} - x_{\text{first}})$ and $x_{\text{last}} + a(x_{\text{last}} - x_{\text{last}-1})$, respectively.

Although the interpolated points are very useful sources of information, they come with an error which is assumed to increase with the distance to the nearest real point due to the local nature of the low-order Taylor expansion. For that reason, we above introduce only two additional points which by the choice of a can be relatively close to explicitly evaluated points. Second, the i th point is provided with an uncertainty σ_i that has the equivalent effect of a weight during the polynomial fitting. For the explicitly calculated points, a unit σ_i is assumed, whereas for the interpolated points, σ_i is calculated as

$$\sigma_i = \frac{1}{\delta_i} \quad (9)$$

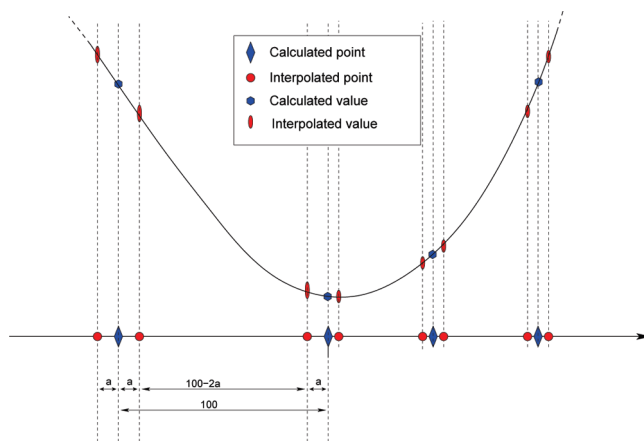


Figure 1. Computed and interpolated points during an ADGA iteration: (blue diamonds) positions of the calculated points; (red dots) positions of the points to be interpolated.

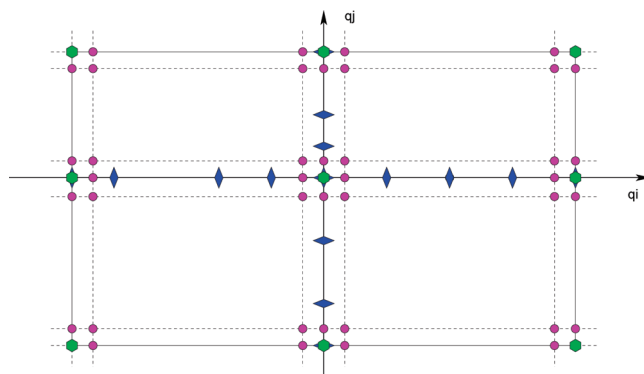


Figure 2. Computed and interpolated points during an ADGA iteration: (green hexagons) positions of the explicitly calculated points for the bidimensional term; (blue diamonds) calculated points on the parental monodimensional surfaces; (magenta dots) points to be interpolated obtained following the a -parameter strategy.

where δ_i depends on the distance between the interpolated point and the calculated points as

$$\delta_i = \sum_k e^{-\lambda d_{ki}/d_{\min}} \quad (10)$$

In eq 10, λ is the decay constant, d_{ki} is the distance between the interpolated point i and the k th calculated point, and d_{\min} is the minimum distance between two calculated points in the mode combination. The effect of this is clearly that increasing the distance to all calculated points will increase σ_i such that the point will have less weight in the fitting. This is in some sense a continuous way of expressing that the local expansions can only have a limited trust radius.

For the multidimensional surfaces a straightforward generalization of this scheme is applied as shown in Figure 2 for a bidimensional term (with the exception that there is no point placed outside of the region defined by the monodimensional boundaries). The points explicitly calculated are green (note that the points on the monodimensional surface that define the direct grid of calculated points are also considered to be explicitly calculated), while the points from a lower order mode coupling are marked with blue diamonds. The interpolated points are shown with magenta dots.

For a point on a multidimensional surface, the δ_i used to define the associated uncertainty is computed according to

$$\delta_i = \sum_k \left(\prod_{q \in mc} e^{-\lambda d_{ki}^q / d_{\min}^q} \right) \quad (11)$$

where q is one of the modes present in the mode combination, λ is the decay constant, d_{ki}^q is the q component of distance between the interpolated point i and the k th calculated point, and d_{\min}^q is the minimum distance between two calculated points in the mode combination.

Preliminary tests demonstrated that the performances of the proposed scheme are only weakly dependent on the exact values of the a and λ parameters (if chosen within a reasonable range), and in the following $a = 0.05$ and $\lambda = 8.0$ will be assumed.

For a complete overview of the method, the maximum order of the polynomial entering in the fitting has to be considered. During a standard ADGA iteration, for each direction in the mode coupling, the maximum degree of the fitting polynomial is set to be the larger even number equal to or smaller than n , with n being the number of points determining the direct grid in that direction. The maximum order then increases with more points up to a user-specified maximum order. In the example shown in Figure 2, which matches a first iteration in the ADGA calculation of a two-mode coupling, there are 3 calculation points for each mode. Under these circumstances, the standard procedure of not using interpolation will set up a maximum order of the polynomial equal to 2 for each mode, and hence, the basis for the fitting will include four terms, namely, $q_i q_j$, $q_i^2 q_j$, $q_i q_j^2$, and $q_i^2 q_j^2$. In order to account for the additional information provided by the interpolated point, it was found adequate to increase the maximum order of the polynomial to four in the first iteration, whereas in the subsequent iterations the standard rule is used. For the multidimensional case it is in addition customary to set a combined maximum polynomial order (max_order), i.e., $q_i^a q_j^b \in \{q_i^a q_j^b \mid a + b \leq \text{max_order}\}$.

2.3.3. Extrapolation. With a somewhat similar setup, as previously described, one can approximate energy values in a mode coupling with no explicit calculation points except those of the limiting mode couplings obtained by setting one of the coordinates to zero. We denote this as an extrapolation as it is an extrapolation from the grid points of a lower coupling grid calculation (say including up to two-mode couplings) to an estimated function for a higher mode coupling (three-mode couplings). It should be noted, however, that it is still a kind of interpolation from a global view of the function.

In this case, the point to be extrapolated, \vec{q} , is given by the direct product of the grid of points of lower dimensionality. The estimated value of the function at the point to be extrapolated is correspondingly obtained as the weighted sum of the result obtained from the Taylor expansions around the projections of this point to the individual mode-coupling surfaces of one lower dimension.

Detailed equations and a number of graphical illustrations of the procedure are given in ref 36. In Figure 3 the strategy for extrapolation of a bidimensional mode coupling is indicated: the computed grid of points (blue diamonds) on

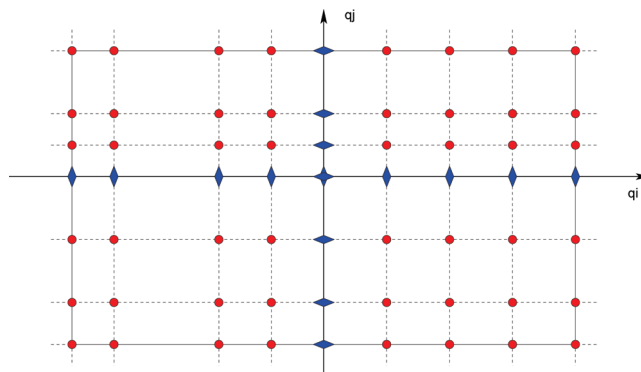


Figure 3. Extrapolation of a bidimensional term: (blue diamonds) positions of the calculated points; (red dots) positions of the points to be extrapolated.

the monodimensional surfaces define a direct product grid of points that will be extrapolated (red dots).

The method, likewise MSI, depends only on an analytical parameter-free weight factor, eq 8, which controls the contributions from each direction of extrapolation. Interestingly, extrapolation is much less dependent on the power of the distance chosen for the weight factors³⁶ and the accuracy of the method is mainly given by the order of the derivatives used in the Taylor series. Should V^{n+1} be represented by an n -variate polynomial, it is easy to prove that the terms of V^{n+1} with powers not higher than the order of derivatives used in the Taylor series are reproduced *exactly*. Other terms are approximated by the aforementioned weighted sum of Taylor expansions. Therefore, when using second-order Taylor expansions one anticipates that pure or mixed linear and quadratic terms (i.e., $q_1 q_2 \dots$, $q_1^2 q_2 \dots$, \dots , $q_1^2 q_2^2 \dots$) are exact in the polynomial representation.

In ref 36 the extrapolation procedure has been successfully applied to a representative set of molecules, showing that the use of first derivatives improves relative to the original PES, V^n , and the use of second derivatives provides a PES with an accuracy comparable to the full calculation.

In the framework of the ADGA, the possibility to extrapolate potential terms from the information collected during construction of the lower dimensionality terms has two applications. The extrapolated PEFs may be used without further refinement to approximate higher mode couplings. Alternatively, the approximated potentials may serve as educated guesses for the “zero”-order $(\rho V)_i$ quantity in the first iteration of the ADGA. The basic extrapolation strategy requires no essential modifications, but there are a few practical differences compared to the previous tests.³⁶ First, the ADGA grid will be small and not regular in contrast to the rich and regular grids for which the extrapolation procedure was tested originally. We expect this to be of minor numerical importance as ADGA per definition should define the grid points to be where there are large contributions and large variations. Furthermore, in accordance with the fact that second-order Taylor expansions provide exact pure and mixed linear and quadratic terms, for each mode in the mode combination a maximum polynomial degree equal to two is adopted in the fitting procedure (recalling that still terms such as $q_1^2 q_2^2 \dots$ are allowed). At this stage, since all the points entering the fitting are extrapolated, all

the weights are identical. Higher order expansion can be requested by the user, but we will throughout use this lower order possibility. This was found satisfactory in preliminary test calculations, and limiting the number of terms in the potential representation will be computationally convenient, especially for larger systems.

2.4. Further Implementational Details: Symmetry and Parallelization. All of the above-mentioned procedures have been implemented in the current version of MidasCpp (Molecular Interactions, Dynamics, and Simulations Chemistry Program Package),⁵⁰ containing both PES and wave function modules. The PES module interacts smoothly with the wave function modules for fast VSCF density calculation during the ADGA calculations and for post-PES vibrational calculations with VSCF, VCI, VMP, VAPT (vibrational autoadjusting perturbation theory),⁵¹ and VCC. The PES module includes interpolation (cubic-splines, modified Shepard), the MS-based extrapolation step, ADGA (with multi-resolution options), as well as the use of point group symmetry and parallelization described very briefly below.

The current version of MidasCpp can exploit point group symmetry to avoid computation of symmetry equivalent structures and generate symmetry pure potentials. The abelian groups are implemented, and implementation takes advantage of the fact that the irreducible representations of the abelian groups are monodimensional. Hence, knowledge of the character table of each group gives the direct effect of the various symmetry operations on the normal coordinates as the effect is multiplication by either +1 or -1. By noting that the normal coordinates are already a set of symmetry-adapted coordinates, it is clear that symmetry-related structures can be found only within the same mode combination. The strategy adopted to exploit molecular symmetry for both energies, properties, and derivatives is as follows. The program analyzes the list of the requested calculations at each ADGA iteration and discards those of symmetry-related structures: only unique structures are computed. Whereas two symmetry-related structures share the same orientation-independent properties (e.g., energy), the rotation matrix between the two structures has to be determined to transform the orientation-dependent properties (e.g., dipole moment components). Derivatives are consistently transformed using the same rotation matrix. The full list of calculations is compiled based on the information in the previous two steps. Furthermore, if the electronic structure program has the capability to recognize and exploit molecular symmetry for a given molecular structure, this feature is used to speed up the corresponding single-point calculation. If the use of symmetry in the single-point calculation requires the program to rotate the molecule into the inertial axes frame and/or the nuclei-specific properties are printed only for symmetry-independent centers, MidasCpp is capable of reconstructing the redundant list of values and reorient the orientation-dependent properties in its coordinate system. In this way MidasCpp can handle several properties such as nuclear magnetic shielding constants, molecular dipole moments (including derivatives), and (hyper)polarizabilities, etc. Finally, we note that symmetry-adapted polynomial functions are used in the fitting and PES representation.

We note that during a specific ADGA iteration, a list of single-point calculations is requested. As the single points are independent, their calculation represents an embarrassingly parallel problem. It is thus possible to setup a very efficient parallelization framework. Our current implementation mimics a master/slaves approach, with the MidasCpp process submitting single-point calculations and collecting the needed results of each calculation. Hybrid approaches are also possible where MidasCpp runs in parallel several electronic structure calculations, each of which runs in parallel.

2.5. On the Relative Cost of the Derivative- vs No-Derivative-Based Calculations. While the use of derivatives is conceptually appealing, derivatives comes with an additional cost. It has previously been discussed how the calculation time in particular modifies the scaling gains obtained by the extrapolation trick.³⁶ However, this was in the context of a fixed and large grid. We now describe how this discussion is modified in important ways in the context of the dynamic ADGA grids, which ultimately will decide if a particular choice of ADGA grid level combined with extrapolation is computationally efficient.

The computational cost of Hessian calculations is, for medium-sized molecules, generally expected to exceed the cost of a energy calculation by a factor $C \times M$. Here, M is the number of modes in the molecule (and for a nonlinear molecule $M = 3N - 6$, and for the purpose of scaling arguments it is not too different from $3N$, with N being the number of atoms). C is some characteristic constant factor relating to the electronic structure method and its implementation, which is anticipated to be on the order of unity. For a gradient calculation, the relative time of calculating the energy and gradient compared to an energy-only calculation is typically a small constant close to 1 for variational wave functions and close to 2 for nonvariational methods such as coupled cluster (CC). Concerning the calculation and use of first derivatives, it is also fair to add that vibrational calculations often require other first-order properties (e.g., dipole moment for calculation of absorption spectra); hence, the gradient is essentially available at very little additional cost.

Clearly, in order to be useful for a reduction of the computational time, the savings in the number of single-point calculations due to the use of derivatives must not to be overwhelmed by the increased cost of each single-point calculation.

If one considers a grid approach where one generates for each mode coupling a direct product grid of points, the cost is dominated by computation of the n -mode couplings where n is the highest coupling level included in the molecular PES. The number of single points needed is then on the order of

$$\binom{M}{n} g_n^n$$

where g_n is the number of single points per direction in generation of the direct grid. If one can extrapolate the higher couplings from the $(n - 1)$ th terms, the required number of single points is on the order of

$$\left(\frac{M}{n-1}\right)g_{n-1}^{(n-1)}$$

For large enough M , this guarantees a reduction in the number of grid points requested on the order of $(M/n)(g_n^n/g_{n-1}^{(n-1)})$. For the gradient extrapolation this is clearly very favorable as the additional cost for computing gradients is small. For the Hessian-based extrapolation the situation is less clear.

Let us for a moment consider the simplest case of the same number of grid points per mode being used in the different mode coupling levels, and thus, $g_n = g_{n-1} = g$, then the reduction in grid points is a factor $(Mg)/(n)$. Taking into account the additional C factor we obtain a ratio in the computational cost of full grid vs Hessian-extrapolated static grid approach as $(g)/(Cn)$. There is a good efficiency gain if the number of grid points per direction is large, but the efficiency gain (if at all a gain) decreases with increasing mode-coupling level n and the factor C . Slightly more general, we can expect a reduction of the total computational cost of a factor $(1/Cn)(g_n^n/g_{n-1}^{(n-1)})$, so there can be significant gain using also Hessians especially for $n = 2$ (thus for the 1M to 2M extrapolation) and when $g_n \approx g_{n-1}$.

ADGA was designed to efficiently address construction of mode couplings through a careful selection of the single points needed by analyzing the vibrational wave function density and the strength of the couplings. In agreement with the expectation that the strength of the coupling decreases with increasing mode-coupling level, the number of grid points is not constant anymore. One can say that the effective number of grid points per dimension decreases with n . For ADGA, the effective g_n can be expected to be larger than 10 for $n = 1$ and 2; for systems with modest three-mode couplings g_3 drops significantly below 10 on average, being often as small as 4 with a minimum of 2. The electronic structure program factor C varies of course with different methods and programs, but it should be on the order of unity; we found it to be around 3 in our applications and tests. This in turn means that the Hessian-based extrapolations can be a savings in the computational time when extrapolating the two-mode couplings from the one-mode grid. However, it will often not be competitive for the two- to three-mode extrapolation, if compared with the efficiency of a pure ADGA on higher mode couplings.

In summary, from scaling perspectives it is clear that gradient extrapolations are always useful in the sense of providing additional information at almost no additional cost. Hessian-based extrapolations can be useful, but it depends more on the case, and relative to an efficient ADGA prediction of the higher mode coupling the relative gain in total CPU time will be modest if at all a gain. We will explore in the tests all options at the two- and three-mode coupling level to obtain some insight in the accuracies that are obtainable and, in the light of the above, the accuracy/cost ratios of the different methods.

3. Computational Details

Construction of PESs requires as input vibrational frequencies and normal coordinates. In the first part of the results

section we adopted Hartree–Fock theory in connection with STO-3G basis sets for calculation of the normal coordinates, vibrational frequencies, and single points needed in construction of the PESs. Whereas this level of theory is far from optimal for obtaining highly accurate surfaces, it allows for a systematic investigation of the parameters controlling integration of the adaptive algorithm with the Shepard’s techniques. In addition, analytic gradients and Hessians are available for the ground state energy, whereas first derivatives are used for the dipole moment components.

In the second part of the results section, we aim at an accurate and cost-effective PES construction, using the insight gained with the above benchmarks. At this stage, we employ coupled-cluster singles and doubles with perturbative triples correction⁵² (CCSD(T)) level of theory in connection with triple- ζ quality basis sets (cc-pVTZ)^{53–55} for geometry optimization and harmonic vibrational analysis. Construction of the analytic form of the potential and property surfaces is achieved with a multiresolution scheme:²⁹ monodimensional PEFs are computed at the CCSD(T)/cc-pVTZ level of theory, whereas bidimensional couplings and extrapolated three-dimensional couplings are constructed by means of CCSD/cc-pVTZ or MP2/cc-pVTZ calculations. All electronic structure calculations have been carried out with the CFOUR program.⁵⁶

Concerning the thresholds used in the ADGA procedure (see ref 28 for details), the monodimensional surfaces are converged with $\epsilon_{\text{rel}} = 5 \times 10^{-3}$ and $\epsilon_{\text{abs}} = 5 \times 10^{-7}$, the bidimensional surfaces are converged with $\epsilon_{\text{rel}} = 3 \times 10^{-2}$ and $\epsilon_{\text{abs}} = 3 \times 10^{-6}$, and the three-dimensional surfaces are converged with $\epsilon_{\text{rel}} = 1 \times 10^{-1}$ and $\epsilon_{\text{abs}} = 1 \times 10^{-5}$. These thresholds ensure that the representation of the PEFs are tightly converged.

The maximum polynomial degree used for fitting of the monodimensional and bidimensional surfaces is 12, while for the three-mode PEFs a maximum polynomial degree of 10 is used.

The boundaries of the monodimensional grids are iteratively determined by requiring that 99.9% of the mean density constructed from the three lowest vibrational states for each vibrational mode is included in the boundaries of the monodimensional grids. For the second part of the PES construction, namely, accurate CCSD(T) surfaces, the latter parameter is set to four.

The one-mode vibrational densities used in the ADGA are obtained from VSCF calculations on the ground vibrational states. The VSCF modals are expanded in a set of distributed Gaussians, generated from a basis set density equal to 0.8; the details for this basis set can be found in ref 28. For the correlated vibrational calculation, the VCC[2pt3] method³⁹ is applied. The lowest 8 VSCF modals per mode are retained in the correlated calculations. Coriolis coupling effects are taken into account by approximating the elements of the effective moment of inertia tensor with their equilibrium values and limiting the operator to a 3-mode operator.

Table 1. Methanimine: Potential Energy Surfaces Constructed with and without Derivative Information^a

no. of calcs potential ^d	96		no derivatives in ADGA ^b			derivatives used in ADGA ^c		
			3438		7731	2880		5354
	1M	1hx2M	2M	2hx3M	3M	2M	2hx3M	3M
MAD(2M) ^d	54.9	4.3	0.0			0.3		
MaxAD(2M) ^d	184.8	10.4	0.0			0.7		
MAD(3M) ^e	48.8	10.0	8.8	0.9	0.0	8.6	1.2	0.9
MaxAD(3M) ^e	130.2	65.1	54.7	2.0	0.0	54.0	3.2	3.0

^a Summary of the mean absolute deviation (MAD) and max absolute deviation (MaxAD) computed for the fundamental frequencies with respect to results obtained with a converged potential. The single-point calculations are carried out at the HF/STO-3G level of theory. The vibrational method adopted is VCC[2pt3]. The values are given in cm^{-1} . ^b Derivatives are not used in the 2M and 3M ADGA iterations. (Derivatives are used in construction of the monodimensional terms and in extrapolation of high mode couplings; see text for details.)

^c Interpolation exploited as in Figure 1. ^d Reference data entering the statistical analysis are obtained with the 2M PES calculated with ADGA without the use of derivatives. ^e Reference data entering the statistical analysis are obtained with the 3M PES calculated with ADGA without the use of derivatives.

4. Results and Discussions

4.1. Convergence Benchmark. In this section we explore the properties and accuracy of the higher order PEFs extrapolated by means of the MS technique as well as the speed up in the convergence of the ADGA when derivative information is exploited. As previously described, the spatial extension of the grids sampling the PEFs is determined during construction of the monodimensional terms. In order to obtain a fair comparison, the potentials termed “with derivatives” and “without derivatives” were forced to share the same monodimensional part (i.e., constructed by exploiting derivatives). This ensures that the observed discrepancies are inherent to the PES qualities of the coupling potentials which is the computationally most demanding and not due to subtle differences in the final calculation (e.g., basis set distribution and extent of sampled space).

The first molecule to be addressed is methanimine (CH_2NH), and the corresponding results are reported in Table 1. Initially we consider calculations where MSI is not used during the ADGA for the two- and three-mode grid parts. From the data, it is possible to determine the relative importance of the truncation level in the n -MCR approach. If one compares the fundamental frequencies obtained from a monodimensional approximation to the PES (column 1M) with the data obtained from converged bidimensional potential, the mean absolute deviation (MAD) from the data sets amounts to 54.9 cm^{-1} while the max absolute deviation (MaxAD) is 184.8 cm^{-1} . Significantly smaller numbers are computed from the comparison of the 2M PES with respect to the 3M counterpart (8.8 and 54.7 cm^{-1} , respectively). Although ADGA efficiently lowers the computational cost associated with construction of higher dimension PEFs, the increase in the number of single-point calculations is still significant: construction of the 1M surfaces requires 96 single points, whereas the 2M and 3M surfaces require 3438 and 7731 points, respectively. On the other hand, the correction obtained with inclusion of the extrapolated surfaces is substantial, for instance, the 1hx2M PES (i.e., the PES obtained with the converged 1M potential corrected with 2M terms obtained by extrapolation using up to Hessians) compares well to the standard ADGA 2M potential with a MAD of 4.3 and a MaxAD of 10.4 cm^{-1} . Hence, with respect to complete neglect of two-mode couplings, an order of magnitude smaller discrepancy is achieved with inclusion

of the extrapolated terms. The same conclusion can be drawn if the results from the 2hx3M and full 3M surfaces are compared, only now the absolute size of the deviations is much smaller.

The previous results pertain to the case where the actual ADGA iterations are carried out without the assistance of the derivatives information. The effect of the use of MSI during the ADGA iterations, as depicted in Figure 1, is presented in Table 1. First, with the use of derivatives, the convergence of the ADGA is achieved with fewer single-point evaluations, indicated by the observation that only 2880 and 5354 single-point calculations are needed for the 2M and 3M PESs, respectively. In spite of the reduction in the single energy points required, the accuracy is comparable. The MAD for the fundamental frequencies computed from these potentials, with respect to the counterpart constructed without MS interpolation, is 0.3 and 0.7 cm^{-1} for the 2M and 3M PESs, respectively. Furthermore, it is worth noticing that the reduction in the number of required single-point evaluations (and derivatives) does not affect the efficiency of the extrapolation scheme. This is shown by the statistical analysis of the results obtained on the 2hx3M PES: the MAD(3M) (deviation relative to 3M) is only 0.3 cm^{-1} larger than the counterpart already commented. Considering the number of single-point calculations, the performance of the 2hx3M PES is remarkable. In spite of the fact that it only requires 2880 single-point calculations, it gives rise to fundamental frequencies that compare with a MAD of 1.2 cm^{-1} (MaxAD 3.2 cm^{-1}) to the results achieved using a 3M PES based on 7731 points.

Concerning the relative accuracy of the calculation with and without MSI in the ADGA exploratory calculation pushing the threshold even lower gives results in between the two, indicating that the larger number of points in the calculation without MSI compensates somewhat for the derivative information provided by the MSI.

The second system investigated in this survey is a trisubstituted methane (CHFCIBr). Table 2 shows the corresponding statistical analysis on the computed fundamental frequencies with different approximations for the PES. Although this molecule has the same number of modes (and mode couplings) as the previous one, it is clear that the inherent complexity of the PES is lower, for instance, the MAD between the frequencies computed with a PES

Table 2. CHFCIBr: Potential Energy Surfaces Constructed with or without Derivative Information^a

no. of calcs	90		no derivatives ^b			derivatives ^c			
			2703		4620	2086		3982	
	potential ^d	1M	1hx2M	2M	2hx3M	3M	2M	2hx3M	3M
MAD(2M) ^d	14.6	2.1	0.0				0.0		
MaxAD(2M) ^d	56.4	13.0	0.0				0.1		
MAD(3M) ^e	13.0	3.0	2.1	0.7	0.0		2.2	0.6	0.3
MaxAD(3M) ^e	48.2	15.9	8.2	1.8	0.0		8.2	1.8	0.8

^a Summary of the mean absolute deviation (MAD) and max absolute deviation (MaxAD) computed for the fundamental frequencies with respect to results obtained with a converged potential. The single-point calculations are carried out at the HF/STO-3G level of theory. The vibrational method adopted is VCC[2pt3]. The values are given in cm^{-1} . ^b Derivatives are not used in the 2M and 3M ADGA iterations. (Derivatives are used in construction of the monodimensional terms and in extrapolation of high mode couplings; see text for details.)

^c Interpolation exploited as in Figure 1. ^d Reference data entering the statistical analysis are obtained with the 2M PES calculated with ADGA without the use of derivatives. ^e Reference data entering the statistical analysis are obtained with the 3M PES calculated with ADGA without the use of derivatives.

Table 3. Oxazole: Potential Energy Surfaces Constructed with or without Derivative Information^a

no. of calcs	154		no derivatives ^b			derivatives ^c			
			8686		33 675	6119		16 379	
	potential ^d	1M	1hx2M	2M	2hx3M	3M	2M	2hx3M	3M
MAD(2M) ^d	37.7	5.0	0.0				0.3		
MaxAD(2M) ^d	164.9	22.7	0.0				0.7		
MAD(3M) ^e	36.0	12.2	9.1	2.1	0.0		8.9	2.0	1.1
MaxAD(3M) ^e	114.3	69.1	50.6	11.0	0.0		49.9	11.6	6.1

^a Summary of the mean absolute deviation (MAD) and max absolute deviation (MaxAD) computed for the fundamental frequencies with respect to the results obtained with a converged potential. The single-point calculations are carried out at the HF/STO-3G level of theory. The vibrational method adopted is VCC[2pt3]. The values are given in cm^{-1} . ^b Derivatives are not used in the 2M and 3M ADGA iterations. (Derivatives are used in construction of the monodimensional terms and in extrapolation of high mode couplings, see text for details.)

^c Interpolation exploited as in Figure 1. ^d Reference data entering the statistical analysis are obtained with the 2M PES calculated with ADGA without the use of derivatives. ^e Reference data entering the statistical analysis are obtained with the 3M PES calculated with ADGA without the use of derivatives.

truncated to the 1M terms and the corresponding data from a 2M potential is equal to 14.6 cm^{-1} . The same applies if one considers the 2M and 3M potentials where the discrepancies are 2.1 and 8.2 cm^{-1} for MAD and MaxAD, respectively. This is a clear indication that the strengths of the 2M and 3M mode couplings are quite low. As expected, with such a situation, ADGA is capable of providing converged surfaces using considerably fewer points compared to the methanimine system. The full 2M construction required 2703 single points, while 4620 points are needed for the 3M PES. Focusing on the Shepard extrapolated surface, the good performances are confirmed: the largest 1hx2M – 2M discrepancy amounts to 13.0 cm^{-1} and drops to 1.8 cm^{-1} if one considers the 2hx3M – 3M case. If Shepard interpolation is used during the ADGA iteration the obtained surfaces are virtually equivalent to the previous one (MaxAD(2M), 0.1 cm^{-1} ; MaxAD(3M), 0.8 cm^{-1}) but a considerable savings in terms of the number of required points is achieved: 2086 instead of 2703 single-point calculations are adequate for obtaining convergence for the 2M surfaces.

The last molecule studied in order to evaluate the accuracy and features of the merging of ADGA and MSI interpolation/extrapolation is oxazole ($\text{C}_3\text{H}_3\text{NO}$). This system represents a somewhat larger system than the previous one with its 18 vibrational degrees of freedom. Following the scheme already presented, the statistical analysis of the fundamental frequencies computed with different PES approximations is provided in Table 3. The evolution of the computed fundamental frequencies with the mode–mode coupling in the potential

is similar to the case of methanimine: a strong dependence on the mode-coupling level of the PES is observed. In fact, the computed fundamental frequencies with a 2M or 3M potential differ by as much as 50 cm^{-1} . On the other hand, when extrapolated PEFs are added to the PES, such discrepancies drop by a factor of 4.5. Furthermore, for this molecule the computational savings associated with the use of derivatives is remarkable: a full 3M potential computed with the ADGA approach requires 33 675 single-point calculations, whereas the ADGA+MS approach lowers the amount to 16 379 with an average error of 1.1 cm^{-1} . Finally, it is noteworthy that the 2hx3M potential gives fundamental frequencies with an average error of 2.0 cm^{-1} in spite of a total request of points equal to 6119.

In this section we investigated the performances of the proposed merging of the ADGA for PES construction with the use of both first- and second-derivative information via MS techniques. We showed that (i) a consistent savings in the total number of single-point calculations is achievable and (ii) extrapolation of higher order coupling terms provides an accurate approximation to the fully converged potential. For oxazole, a modest static grid based on 16, 144 (12×12), and 216 ($6 \times 6 \times 6$) points for monodimensional, bidimensional, and tridimensional mode couplings, respectively, requires, after symmetry screening, 135 897 electronic calculations, putting the gain of the combined ADGA/MS approaches in perspective.

As discussed in section 2.5, despite the significant lowering of the number of grid points, the use of second derivatives can be disfavored by the high computational cost of second

Table 4. Use of Gradients in the Construction of Potential Energy Surfaces: Summary of the Mean Absolute Deviation (MAD) and Max Absolute Deviation (MaxAD) Computed for the Fundamental Frequencies with Respect to Results Obtained with Converged Potentials^a

no. of calcs	methanimine					CHFCIBr					oxazole				
	98		3370		7017	90		2691		4739	154		8530		29028
PES	1M	1gx2M	2M	2gx3M	3M	1M	1gx2M	2M	2gx3M	3M	1M	1gx2M	2M	2gx3M	3M
MAD(1M) ^b	0.2					0.1					0.2				
MaxAD(1M) ^b	0.4					0.2					0.4				
MAD(2M) ^c	54.7	56.6	0.1			14.5	19.9	0.0			37.5	37.3	0.3		
MaxAD(2M) ^c	184.5	141.0	0.1			56.3	60.8	0.1			164.5	123.3	1.2		
MAD(3M) ^d			8.8	3.6	1.0			2.1	1.8	0.2			9.3	3.0	1.3
MaxAD(3M) ^d			54.8	9.3	3.0			8.3	5.2	0.7			50.3	19.7	4.3

^a Reference values computed as in Tables 1, 2, and 3. The single-point calculations are carried out at the HF/STO-3G level of theory. The vibrational method adopted is VCC[2pt3]. The values are given in cm⁻¹. ^b The reference data entering the statistical analysis are obtained with the 1M PES calculated with ADGA without the use of derivatives. ^c The reference data entering the statistical analysis are obtained with the 2M PES calculated with ADGA without the use of derivatives. ^d The reference data entering the statistical analysis are obtained with the converged 3M PES calculated with ADGA without the use of derivatives.

derivatives. Thus, while there can be a gain compared to the static grid three-mode calculation, ADGA reduces in effect the number of grid points per dimension of a corresponding explicit three-mode calculation. As a result, the additional savings in the total number of single points obtained by the Hessians in the 2hx3M calculation far from justifies the extra cost of the calculation of the Hessian for the present set of molecules and calculations (i.e., the total time is actually longer).

So far we have discussed the case where, for each single-point calculation, both gradient and Hessian are available. Having illustrated that good accuracy can be obtained and that significant reductions in the number of single-point calculations can be obtained from extrapolation procedures, we will now address the efficiency of our procedure in the case where only gradient information is used. The gradients often come with modest extra effort compared to an energy calculation, while the Hessian requires substantial extra effort. In Table 4, the statistical analysis on the fundamental frequencies computed for various PESs is investigated. Note that the monodimensional PEFs are constructed ex novo using only gradients, which results in a negligible difference with respect to the results where both Hessians and gradients are used. Using only gradients in the extrapolations of the two-mode PEFs does not provide significant improvement with respect to the pure 1M potentials and is obviously useless. On the other hand, inclusion of the three-mode extrapolated corrections significantly improves the agreement with the full 3M potentials. The latter observations are in agreement with the results in ref 36. For instance, in the case of methanimine, the MaxAD(3M) drops from 54.8 to 9.3 cm⁻¹ when including the extrapolated terms. In the case of oxazole, the MaxAD(3M) residual error is somehow larger (19.7 cm⁻¹); nevertheless, the average error is only 3.0 cm⁻¹. This suggests that the essential part of the 3-mode couplings is well described by the extrapolation procedure, though of course not as accurate as with the extrapolations using up to Hessians. Finally, one notices that the use of gradients in combination with the ADGA provides a small improvement with respect to the number of single points needed for convergence of the PES, but the savings hardly exceeds 10%.

In conclusion, although the accuracy achieved with the use of second derivatives in the MS interpolation/extrapolation

is not fully met if one uses only first derivatives, inclusion of gradient information during construction of a PES is found to be advantageous, especially for extrapolation of the 3-mode coupling corrections, at least for these fairly rigid systems. Thus, the ADGA[2gx3M] potential is certainly a cost-efficient approach and taking into account the much higher cost of Hessians the ADGA[2gx3M] is likely to be more useful in production calculations than ADGA[2hx3M].

4.2. Methanimine and Oxazole: Comparison with Experimental Spectra. The experimental vibrational frequencies of methanimine are taken from refs 57 and 58, while for oxazole, the data in the Computational Chemistry Comparison and Benchmark Database (CCCBDB) are used,⁵⁹ maintained by the National Institute of Standards and Technology, except for the frequencies ν_6 and $\nu_8-\nu_{17}$, which are available in a recent high-resolution infrared study.⁶⁰

In Table 5 we report fundamental frequencies and one combination band calculated with a 3M potential obtained as ADGA[2hx3M] where 1M:CCSD(T)/cc-pVTZ//2hx3M:CCSD/cc-pVTZ. The results presented clearly demonstrate that the ADGA combined with the MS techniques is a robust methodology which provides accurate PESs when based on high-quality single-point calculations. The computed frequencies are found within 8 cm⁻¹ from the experimental values, and the statistical analysis of the results gives a MAD 3.7 cm⁻¹, respectively. We note in passing that for ν_2 and ν_3 there is significant mixing of the fundamental with a combination band ($\nu_4 + \nu_6$) and an overtone ($2\nu_5$), respectively. As observed by De Oliveira et al., these mixings are so severe that assignment of any of the observed peaks to match a pure fundamental is inappropriate.⁶¹

In addition, extrapolation of the 3-mode coupling is addressed by means of ADGA[2gx3M] potentials where 1M:CCSD(T)/cc-pVTZ//2gx3M:MP2/cc-pVTZ or 1M:CCSD(T)/cc-pVTZ//2gx3M:CCSD/cc-pVTZ. In all cases a good agreement with the experimental values is found (MAD 3.0–3.5; MaxAD ca. 10.0 cm⁻¹), confirming that the extrapolated 3M PEFs using only first-derivative information are sufficiently accurate to be highly useful. It is worth mentioning that a corresponding vibrational calculation leaving out extrapolated 3-mode couplings gives significantly less accurate results, as evident from the MAD and MaxAD, which amounts to 10.5 and 62.5 cm⁻¹, respectively. In

Table 5. Methanimine: Calculated Frequencies with Respect to the Experimental Counterpart^a

mode	symmetry	experimental ^b	calculated ^c ADGA[2hx3M]	calculated ^d ADGA[2gx3M]	calculated ^e ADGA[2gx3M]
ν_1	A'	3262.6	3265.2 (2.6)	3263.4 (0.8)	3263.4 (0.8)
$\nu_2 - \nu_4\nu_6$	A'	3024.5	3032.3 (7.8)	3024.2 (-0.3)	3027.7 (3.2)
$\nu_4\nu_6 + \nu_2$	A'		2965.8 (-)	2957.9 (-)	2954.9 (-)
$\nu_3 + 2\nu_5$	A'	2914.2	2916.8 (2.6)	2907.9 (-6.3)	2906.0 (-8.2)
$2\nu_5 - \nu_3$	A'	2885.0	2889.4 (4.4)	2885.1 (0.1)	2885.7 (0.7)
ν_4	A'	1638.3	1634.6 (-3.7)	1632.5 (-5.8)	1632.3 (-6.0)
ν_5	A'	1452.0	1451.9 (-0.1)	1449.8 (-2.2)	1449.4 (-2.6)
ν_6	A'	1344.3	1351.1 (6.8)	1346.8 (2.5)	1345.7 (1.4)
ν_7	A'	1058.2	1059.4 (1.2)	1057.4 (-0.8)	1057.0 (-1.2)
ν_8	A''	1127.0	1131.3 (4.3)	1125.6 (-1.4)	1125.8 (-1.2)
ν_9	A''	1060.8	1056.7 (-4.1)	1050.8 (-10.0)	1050.7 (-10.1)
MAD			3.7	3.0	3.5
MaxAD			7.8	10.0	10.1

^a The discrepancy with respect to the experimental values is given in parentheses; Mean absolute deviation (MAD) and maximum absolute deviation (MaxAD) are reported. The values are given in cm^{-1} . ^b Experimental values from ref 59. ^c Vibrational calculation: VCC[2pt3] on a ADGA[2hx3M] potential (1M:CCSD(T)/cc-pVTZ//2hx3M:CCSD/cc-pVTZ see text for details). ^d Vibrational calculation: VCC[2pt3] on a ADGA[2gx3M] potential (1M:CCSD(T)/cc-pVTZ//2gx3M:CCSD/cc-pVTZ see text for details). ^e Vibrational calculation: VCC[2pt3] on a ADGA[2gx3M] potential (1M:CCSD(T)/cc-pVTZ//2gx3M:MP2/cc-pVTZ see text for details).

addition, the physical nature of the converged states can be completely different: In the case of the ν_2 fundamental excitation, the two-mode coupling potential is not capable of providing the nonzero coupling that is required to obtain the significant mixing that is found using the 3M surfaces.

Overall, our results show similar accuracy as the data obtained by Rauhut with vibrational configuration interaction VCI(SDTQ) on a 3M potential based on (large basis set and F12) CCSD(T)⁶² and by De Oliveira et al. with vibrational perturbation theory on a high-quality CCSD(T) quartic force field.⁶¹

For oxazole, the hybrid potential ADGA[2gx3M] where 1M:CCSD(T)/cc-pVTZ//2gx3M:MP2/cc-pVTZ has been constructed. Such a PES requires ca. 170 single-point evaluations at CCSD(T)/cc-pVTZ level of theory for the monodimensional terms, while about 11 600 MP2/cc-pVTZ single-point (including gradient) calculations are needed for the 2gx3M part.

The fundamental vibrational frequencies of oxazole computed at the VCC[2pt3] level of theory are shown in Table 6. The comparison with the experimental data is fairly good, and although the MAD (7.1 cm^{-1}) is slightly larger than in the case of methanimine, the largest error is limited to -15.5 cm^{-1} for the ν_9 frequency. For comparison, it is worth mentioning that the frequencies computed by VCC[2pt3] using the ADGA[1M] PES, constructed with CCSD(T)/cc-pVTZ single-point calculations, have a MaxAD with respect to the experimental results in excess of 108 cm^{-1} . If the extrapolated 3M corrections are excluded from the hybrid PES ADGA [2M] (1M:CCSD(T)/cc-pVTZ//2M:MP2/cc-pVTZ), a maximum discrepancy of 47.7 cm^{-1} is found. Once again, this confirms the importance of the inclusion of the 3M PEFs in the approximated PES, and it corroborates the thesis that the 3M corrections extrapolated by means of gradient information provide a qualitative improvement over the 2M PES.

A summary for the combined effect of using approximated treatment of the triple excitations in the wave function part and approximated 3-mode couplings in the potential is given in Table 7.

Table 6. Oxazole: Calculated Fundamental Frequencies and Comparison with the Experimental Data^a

mode	symmetry	ADGA[2gx3M]	
		exp ^b	calcd ^c
ν_1	A'	3170.0	3174.9 (4.9)
ν_2	A'	3144.0	3158.6 (14.6)
ν_3	A'	3141.0	3142.6 (1.6)
ν_4	A'	1537.0	1534.8 (-2.2)
ν_5	A'	1504.0	1492.4 (-11.6)
ν_6	A'	1329.8	1319.0 (-10.8)
ν_7	A'	1252.0	1239.3 (-12.7)
ν_8	A'	1142.5	1136.7 (-5.8)
ν_9	A'	1091.1	1075.6 (-15.5)
ν_{10}	A'	1081.3	1084.3 (3.0)
ν_{11}	A'	1051.8	1044.2 (-7.6)
ν_{12}	A'	909.3	903.4 (-5.9)
ν_{13}	A'	899.3	892.9 (-6.4)
ν_{14}	A''	858.2	851.7 (-6.5)
ν_{15}	A''	832.0	821.5 (-10.5)
ν_{16}	A''	749.3	747.0 (-2.3)
ν_{17}	A''	646.4	642.1 (-4.3)
ν_{18}	A''	607.0	605.4 (-1.6)
MAD			7.1
MaxAD			15.5

^a The discrepancy with respect to the experimental values is given in parentheses; mean absolute deviation (MAD) and maximum absolute deviation (MaxAD) are reported. The values are given in cm^{-1} . ^b Experimental values from ref 59. ^c Vibrational calculation: VCC[2pt3] on a ADGA[2gx3M] potential (1M:CCSD(T)/cc-pVTZ//2gx3M:MP2/cc-pVTZ; see text for details).

The data confirms that the level of complexity in the construction of the PES and in the vibrational calculation has to match somewhat from an accuracy/efficiency perspective, e.g., the results indicate that for a given potential including up to m -mode coupling, the vibrational coupled cluster parametrization should include at least m levels of excitations to provide a converged result. The most consistent improvement is obtained when both excitation space and potential is improved from the two-mode coupling to three-mode coupling. This observation offers a useful rule of thumb for the definition of a cost-effective set up for vibrational calculations. On the other hand, we previously argued that approximate inclusion of three-mode couplings may be good enough in the potential and in the wave function as also supported by the summarized data. In this respect, combina-

Table 7. Effect of the 3-Mode Couplings in the Wavefunction and PES^a

	VCC[2]	VCC[2pt3]	VCC[3]
methanimine			
ADGA[2M] ^b	10.5 (63.3)	10.7 (63.7)	10.7 (63.7)
ADGA[2gx3M] ^c	3.9 (14.3)	3.5 (10.1)	3.3 (11.3)
oxazole			
ADGA[2M] ^b	8.3 (47.7)	8.0 (47.7)	
ADGA[2gx3M] ^c	5.9 (24.1)	7.1 (15.5)	

^a The discrepancy with respect to the experimental values is given; mean absolute deviations (maximum absolute deviation) are reported. The values are given in cm⁻¹. ^b 1M:CCSD(T)/cc-pVTZ//2M:MP2/cc-pVTZ. ^c 1M:CCSD(T)/cc-pVTZ//2gx3M:MP2/cc-pVTZ.

tion of the VCC[2pt3] parametrization of the wave function with a potential including approximate 3-mode couplings appears very promising. We note in passing that the above comments applies for vibrational coupled-cluster response calculations of fundamental vibrations. The excitation space for a vibrational configuration interaction response calculation or similarly, when the VCI excitation space is defined relative to the ground state, must be larger to obtain a similar accuracy. For higher excited states and combination bands higher excitation levels are generally expected to be more important also for VCC calculations.

5. Summary

We described the combined use of the adaptive density-guided approach and the MS interpolation/extrapolation techniques in construction of potential energy surfaces for vibrational calculations. The procedure has been applied to three molecules (methanimine, trisubstituted methane, and oxazole) in exploratory calculations and in calculations aiming at comparison with experiment. We have shown that the ADGA in concert with MS interpolation and extrapolation and a multiresolution approach provides a cost-effective route to access high-quality PES for use in explicit anharmonic vibrational calculations. Comparison with experimental data for methanimine and oxazole using ADGA[2gx3M] and ADGA[2hx3M] potentials constructed on the basis of CCSD(T), CCSD, and MP2 calculations give encouraging results.

It was shown that purely extrapolated higher order mode-combination terms capture a large part of the contribution to the fully converged surfaces. A few more detailed conclusions are in place: The accuracy of the two-mode couplings from the 1M grids is remarkable if Hessians are available but not useful when only gradients are used in the extrapolation. On the other hand, in the extrapolation from two- to three-mode couplings very good results are found in either case. From a computational point of view, it seems that the cost associated with calculation of the second derivatives makes the extrapolation using Hessians for three and higher mode couplings too costly to be competitive in the present setup. The use of gradients, on the other hand, is cost efficient and provides a substantial improvement relative to complete neglect of three-mode couplings. Taking into account both accuracy and efficiency the following practical hierarchy of PES construction protocols are suggested for further studies in the context of ADGA: ADGA[1M],

ADGA[1hx2M], ADGA[2M], ADGA[2gx3M], ADGA[3M], ADGA[3gx4M], ... In addition, we also anticipate that the gradient-based extrapolated representation of high mode couplings can be used in future studies using screening techniques of some sort, e.g., the extrapolated surfaces are used as they are for most couplings, while those few couplings that were estimated to be particularly important are further refined by explicit construction.

Certainly, the possibility to obtain three-mode couplings with only two-mode grids is a unique opportunity especially if one considers that gradient information is available with very little extra cost when computing first-order properties (e.g., dipole moments) besides the energy. For systems whose size usually precludes a robust ab initio treatment including three-mode couplings the combined use of, e.g., ADGA[2gx3M] and VCC[2pt3] as done here may turn out to be the only realistic option. Thus, it is hoped that this work can pave the way for more accurate calculations on larger molecules, where calculations have been limited to approaches including only up to two-mode couplings.

Acknowledgment. This work was supported by the Lundbeck Foundation, the Danish National Research Foundation, the Danish Center for Scientific Computing (DCSC), and EUROHORCs through a EURYI award.

References

- (1) Bowman, J. M. *J. Chem. Phys.* **1978**, *68*, 608.
- (2) Bowman, J. M. *Acc. Chem. Res.* **1986**, *19*, 202.
- (3) Gerber, R. B.; Ratner, M. A. *Adv. Chem. Phys.* **1988**, *70*, 97.
- (4) Hansen, M. B.; Sparta, M.; Seidler, P.; Christiansen, O.; Toffoli, D. *J. Chem. Theory Comput.* **2010**, *6*, 235.
- (5) Norris, L. S.; Ratner, M. A.; Roitberg, A. E.; Gerber, R. B. *J. Chem. Phys.* **1996**, *105*, 11261.
- (6) Jung, J. O.; Gerber, R. B. *J. Chem. Phys.* **1996**, *105*, 10332.
- (7) Chaban, G. M.; Jung, J. O.; Gerber, R. B. *J. Chem. Phys.* **1999**, *111*, 1823.
- (8) Christiansen, O. *J. Chem. Phys.* **2003**, *119*, 5773.
- (9) Matsunaga, N.; Chaban, G. M.; Gerber, R. B. *J. Chem. Phys.* **2002**, *117*, 3541.
- (10) Yagi, K.; Hirata, S.; Hirao, K. *J. Chem. Phys.* **2007**, *127*, 034111.
- (11) Bowman, J. M.; Christoffel, K.; Tobin, F. *J. Phys. Chem.* **1979**, *83*, 905.
- (12) Christoffel, K. M.; Bowman, J. M. *Chem. Phys. Lett.* **1982**, *85*, 220.
- (13) Carter, S.; Bowman, J. M.; Handy, N. C. *Theor. Chem. Acc.* **1998**, *100*, 191.
- (14) Christiansen, O. *J. Chem. Phys.* **2004**, *120*, 2149.
- (15) Rauhut, G. *J. Chem. Phys.* **2004**, *121*, 9313.
- (16) Begue, D.; Gohaud, N.; Pouchan, C.; Cassam-Chenai, P.; Lievin, J. *J. Chem. Phys.* **2007**, *127*, 164115.
- (17) Christiansen, O. *J. Chem. Phys.* **2005**, *122*, 194105.
- (18) Seidler, P.; Christiansen, O. *J. Chem. Phys.* **2007**, *126*, 204101.

- (19) Carter, S.; Culik, S. J.; Bowman, J. M. *J. Chem. Phys.* **1997**, *107*, 10458.
- (20) Gerber, R.; Jung, J. In *The vibrational self-consistent field approach and extensions: Method and applications to spectroscopy of large molecules and clusters*; Jensen, P., Bunker, P. R., Eds.; Wiley: Chichester, 2000; pp 365–390.
- (21) Bowman, J. M.; Carter, S.; Huang, X. C. *Int. Rev. Phys. Chem.* **2003**, *22*, 533.
- (22) Benoit, D. M. *J. Chem. Phys.* **2004**, *120*, 562, and references therein.
- (23) Kongsted, J.; Christiansen, O. *J. Chem. Phys.* **2006**, *125*, 124108.
- (24) Yagi, K.; Hirata, S.; Hirao, K. *Theor. Chem. Acc.* **2007**, *118*, 681.
- (25) Toffoli, D.; Kongsted, J.; Christiansen, O. *J. Chem. Phys.* **2007**, *127*, 204106.
- (26) Scribano, Y.; Benoit, D. *J. Chem. Phys.* **2007**, *127*, 164118.
- (27) Hirata, S.; Yagi, K.; Perera, S.; Yamazaki, S.; Hirao, K. *J. Chem. Phys.* **2008**, *128*, 214305.
- (28) Sparta, M.; Toffoli, D.; Christiansen, O. *Theor. Chem. Acc.* **2009**, *123*, 413.
- (29) Sparta, M.; Høyvik, I.-M.; Toffoli, D.; Christiansen, O. *J. Phys. Chem. A* **2009**, *113*, 8712.
- (30) Jakowski, J.; Sumner, I.; Iyengar, S. S. *J. Chem. Theory Comput.* **2006**, *2*, 1203.
- (31) Sumner, I.; Iyengar, S. S. *J. Phys. Chem. A* **2007**, *111*, 10313.
- (32) Manzhos, S.; Carrington, T. *J. Chem. Phys.* **2006**, *125*, 084109.
- (33) Manzhos, S.; Carrington, T., Jr. *J. Chem. Phys.* **2008**, *129*, 224104.
- (34) Dawes, R.; Thompson, D. L.; Guo, Y.; Wagner, A. F.; Minkoff, M. *J. Chem. Phys.* **2007**, *126*, 184108.
- (35) Dawes, R.; Thompson, D. L.; Wagner, A. F.; Minkoff, M. *J. Chem. Phys.* **2008**, *128*, 084107.
- (36) Matito, E.; Toffoli, D.; Christiansen, O. *J. Chem. Phys.* **2009**, *130*, 134104.
- (37) Rauhut, G.; Hartke, B. *J. Chem. Phys.* **2009**, *131*, 014108.
- (38) Seidler, P.; Christiansen, O. *J. Chem. Phys.* **2009**, *131*, 234109.
- (39) Seidler, P.; Matito, E.; Christiansen, O. *J. Chem. Phys.* **2009**, *131*, 034115.
- (40) Watson, J. K. G. *Mol. Phys.* **1968**, *15*, 479.
- (41) Except for the fact that the multidimensional grids are not allowed to extend beyond the boundaries defined by the corresponding monodimensional ones.
- (42) Hrenar, T.; Werner, H.; Rauhut, G. *Phys. Chem. Chem. Phys.* **2005**, *7*, 3123.
- (43) Pflüger, K.; Paulus, M.; Jagiella, S.; Burkert, T.; Rauhut, G. *Theor. Chem. Acc.* **2005**, *114*, 327.
- (44) Rodriguez-Garcia, V.; Hirata, S.; Yagi, K.; Hirao, K.; Taketsugu, T.; Schweigert, I.; Tasumi, M. *J. Chem. Phys.* **2007**, *126*, 124303.
- (45) Yagi, K.; Taketsugu, T.; Hirao, K. *J. Chem. Phys.* **2002**, *116*, 3963.
- (46) Yagi, K.; Oyanagi, C.; Taketsugu, T.; Hirao, K. *J. Chem. Phys.* **2003**, *118*, 1653.
- (47) Oyanagi, C.; Yagi, K.; Taketsugu, T.; Hirao, K. *J. Chem. Phys.* **2006**, *124*, 064311.
- (48) Evenhuis, C.; Manthe, U. *J. Chem. Phys.* **2008**, *129*, 024104.
- (49) Carbonniere, P.; Begue, D.; Dargelos, A.; Pouchan, C. *Chem. Phys.* **2004**, *300*, 41.
- (50) MidasCpp (Molecular Interactions, dynamics and simulation Chemistry program package in C++), 2007; <http://www.chem.au.dk/midas>.
- (51) Matito, E.; Barroso, J. M.; Besalú, E.; Christiansen, O.; Luis, J. M. *Theor. Chem. Acc.* **2009**, *123*, 41.
- (52) Raghavachari, K.; Trucks, G. W.; Pople, J. A.; Headgordon, M. *Chem. Phys. Lett.* **1989**, *157*, 479.
- (53) Dunning, T. H. *J. Chem. Phys.* **1989**, *90*, 1007.
- (54) Kendall, R.; Dunning, T.; Harrison, R. *J. Chem. Phys.* **1992**, *96*, 6769.
- (55) Woon, D.; Dunning, T. *J. Chem. Phys.* **1993**, *98*, 1358.
- (56) Stanton, J.; Gauss, J.; Harding, M.; Szalay, P. *CFOUR, Coupled-Cluster techniques for Computational Chemistry, a quantum-chemical program package*; 2009; see <http://www.cfour.de>.
- (57) Halonen, L.; Duxbury, G. *J. Chem. Phys.* **1985**, *83*, 2091.
- (58) Halonen, L.; Duxbury, G. *Chem. Phys. Lett.* **1985**, *118*, 246.
- (59) Johnson III, R. D. *NIST Computational Chemistry Comparison and Benchmark Database, NIST Standard Reference Database Number 101 Release 14*, 2006; <http://srdata.nist.gov/cccbdb>.
- (60) Hegelund, F.; Larsen, R. W.; Palmer, M. H. *J. Mol. Spectrosc.* **2007**, *241*, 26.
- (61) De Oliveira, G.; Martin, J.; Silwal, I.; Liebman, J. J. *Comput. Chem.* **2001**, *22*, 1297.
- (62) Rauhut, G.; Knizia, G.; Werner, H. *J. Chem. Phys.* **2009**, *130*, 054105.

CT100229F